Int. J. Electrochem. Sci., 14 **(2019)** 6209 – 6222, doi: 10.20964/2019.07.35

International Journal of
ELECTROCHEMICAL
SCIENCE
www.electrochemsci.org

Corrosion of N80 Steel in a Concentrated Tetrapotassium Pyrophosphate Solution and Corrosion Control by Vanadates

Jingmao Zhao[1,2,*], *Qiuxiang Yang*[1], *Chen Zhang*[1,3], *Yuwu Wang*[1]

[1] College of Material Science and Engineering, Beijing University of Chemical Technology, Beijing 100029, China
[2] Beijing Key Laboratory of Electrochemical Process and Technology for Materials, Beijing 100029, China
[3] South China Branch, Sinopec Sales Co., Ltd., Guangzhou 510620, China
Correspondence
[*]E-mail: jingmaozhao@126.com

Received: 9 September 2018 / *Accepted:* 25 October 2018 / *Published:* 10 June 2019

The main purpose of this work is to study the corrosion of N80 steel in a concentrated tetrapotassium pyrophosphate (TKPP) solution at different temperatures and to evaluate the corrosion inhibition performance of relevant chemicals for N80 steel in this solution. This study employed the methods of weight loss, potentiodynamic polarization, electrochemical impedance spectroscopy (EIS), and X-ray photoelectron spectroscopy (XPS). The temperature had a significant influence on the corrosion rate of N80 in solution. Specifically, the corrosion rate was moderate at low temperatures, but increased dramatically when the temperature exceeded 90 °C. At a temperature of 120 °C, the rate was as high as 731 mpy. Among the chemicals investigated, dichromates and vanadates showed excellent inhibition performance. The inhibition induced by vanadates was mainly due to the promotion of carbon steel passivation. In the presence of 0.5 wt. % vanadate, the corrosion rate of N80 steel can be controlled to less than 3 mpy at a temperature of 120 °C.

Keywords: TKPP, corrosion inhibitor, N80 steel, vanadate

1. INTRODUCTION

Oil/gas well control is one of the most concerning issues during drilling operations and processes. When the well penetrates a high pressure gas-producing formation, the formation fluid and gas enter the wellbore and mix with the drilling mud, and the density is significantly reduced by the gas influx. As a result, the pressure of the hydrostatic head on the well is reduced to less than that of

the formation pressure, which might lead to a blowout with severe consequences, including the loss of valuable resources, irreversible damage to the environment, ruined equipment, and most importantly, loss of the safety and lives of the personnel on the drilling rig [1-3]. Hence, a fluid with a sufficiently high density is needed to pump to the wellbore to balance the formation pressure.

At present, high density liquids used in oil wells can be divided into three categories. The first category includes high density mud mixed with weighting agents, such as barium sulfate, magnetite, ceramic powder, manganese ore powder, and other inorganic materials. This type of mud has a density of up to 2.6 g/cm^3. The second category includes solid-free brines, such as solutions of calcium bromide, zinc bromide, zinc chloride, and formate salts. Although potassium formate solution is less corrosive, its highest density is only 1.54 g/cm^3. The density of bromide solution can be as high as 2.3 g/cm^3, but bromide solution is expensive and can cause severe corrosion of completion equipment and production tubing [4]. The mechanism of corrosion from heavy brines is mostly oxygen induced corrosion. The corrosion from brine increases with increasing temperature. Moreover, heavy brines are often acidic. For example, the pH value of 17 PPG $ZnBr_2$ brine is 4.92, which decreases with increasing brine density. In general, a lower pH brine is much more corrosive than a higher pH brine [5]. Corrosion from brine fluid can be inhibited with an oxygen scavenger while a filming amine is used for CO_2 corrosion protection [6]. However, a study by Smart showed that the corrosion rates of iron were lower in bromide-containing solutions than in chloride solutions. On the other hand, lower corrosion rates were observed in calcium-containing halide solutions than in zinc halide solutions [7]. The third category includes high density water-in-oil liquids with densities from 1.40-2.0 g/cm^3 that are formulated with high density brine solutions, emulsifiers, related oils, and if necessary, solid weighting materials. The drawbacks of this type of high density liquid include poor temperature resistance and negative environmental impacts.

Tetrapotassium pyrophosphate ($K_4O_7P_2$), or TKPP, is a commercial chemical produced by many major companies throughout the world. TKPP is commercially available as a free flowing, white, granular solid. TKPP has been certified by the U. S. Department of Transportation as a nontoxic compound. TKPP can dissolve in water readily with a saturated solubility of 187 g/100 g water at 25 °C and a density as high as 1.74 g/cm^3. Therefore, TKPP has the potential to be used for high density well drilling as completion or workover fluid.

However, studies regarding the corrosiveness of TKPP solution have rarely been reported in the literature, especially regarding influence factors such as temperature and solution chemistry. Patton and Corley reported that the corrosion rates measured for TKPP solutions at 194 °F were as low as 2 mpy [8]. The corrosion rate at 400 °F was 14 mpy for 1020 steel coupons exposed to 14.5 PPG TKPP solutions for 60 days. Except for this research article, there is no other available literature regarding iron corrosion in concentrated TKPP solutions or suppression of the corrosion using corrosion inhibitors.

N80 steel is widely used for manufacturing down-hole tubulars, casings and ground transmission pipelines in oil and gas fields. Thus, in this work, the corrosion behaviors of N80 steel in concentrated TKPP solutions with and without various inhibitors were investigated by using weight loss, electrochemical measurements, scanning electron microscopy (SEM) and X-ray photoelectron spectroscopy (XPS).

2. EXPERIMENTAL

2.1. Materials and sample preparation

A 50 wt. % TKPP solution was prepared with tap water and commercial TKPP with a purity of 98 %. Analytical reagent compounds including molybdate, tungstate, vanadate, dichromate, nitrite, phosphate, silicate and acrylamide were selected as corrosion inhibitors.

The material studied was an N80 steel with the following chemical composition (wt. %): C 0.24, Mn 1.19, Si 0.22, P 0.013, S 0.004, Cr 0.036, Mo 0.021, Ni 0.028, V 0.017, Cu 0.019 and Fe bal. The steel was cut into specimens measuring 50 mm×10 mm×3 mm for the weight loss tests and 10 mm×10 mm×3 mm for the electrochemical measurements. The specimens were polished with silicon carbide abrasive paper of up to 1500 grit in water, then degreased in acetone, rinsed with ethanol and dried in cold air before use.

2.2 Weight loss method

The specimens were immersed in test solutions of 500 mL with and without inhibitors for 3 days. The tests at temperatures lower than 100 °C were performed in a water bath and an autoclave at a temperature of 120 °C. Three identical specimens were used for each test to measure the average weight loss. The specimens were weighed before and after the tests using an analytical balance with a precision of 0.1 mg. The surface corrosion products were removed by immersing the specimens in 15 wt. % HCl + 1 wt % T-90 (an acidizing corrosion inhibitor) for 5 min (using absorbent cotton to wipe off the surface). The corrosion rate and the inhibition efficiency (IE %) of the steel were calculated according to the equations in reference [9].

2.3 Electrochemical studies

The electrochemical measurements were performed using a Gamry Interface 1000 electrochemical system with a glass cell with 200 mL 50 wt. % TKPP solution at a pH of 14.33. The cell was equipped with three electrodes with N80 steel as the working electrode, Pt foil as the counter electrode, and a saturated calomel electrode (SCE) with a Luggin capillary salt bridge as the reference electrode.

The potentiodynamic polarization experiments were initiated after the working electrode was immersed for 1 h in the solution, which allowed the electrode to reach a stable state. The potential was scanned from −200 to +1200 mV vs. open circuit potential (OCP) at a scan rate of 0.167 mV s^{-1}, and the potentials reported in this paper are all in reference to the SCE.

The electrochemical impedance spectroscopy (EIS) measurements were conducted after 1 h of immersion in the solution at OCP with an AC amplitude of 5 mV in the frequency range from 100 kHz to 10 MHz. Thirty frequency points logarithmically spaced throughout the frequency range were measured.

At least three electrochemical measurements were performed under each experimental condition to ensure the repeatability of the experiments.

3. RESULTS AND DISCUSSION

3.1 Corrosion behaviors of N80 steel in 50 wt. % TKPP solution

3.1.1 Weight loss studies

Table 1. Corrosion rates of N80 steel at different temperatures

Temperature (°C)	Corrosion rate (mpy)
30	2.4
60	2.9
90	10.6
120	731.0

Table 1 lists the corrosion rates of the N80 steel in the test solution without any inhibitor at different temperatures including 30, 60, 90, and 120 °C. Table 1 shows that the corrosion rate of N80 steel is mild when the temperature is lower than 90 °C, whereas the corrosion rate increases considerably when the temperature exceeds 90 °C. Moreover, the corrosion rate dramatically increases to 731 mpy at 120 °C. This result is significantly different from previous results, possibly due to the different type of steel used [8].

A 50 wt. % TKPP solution is a strong alkali solution with pH value of 14.33. At low temperature, this solution can form a protective film of corrosion products such as iron pyrophosphate on a steel surface. Therefore, the corrosion of carbon steel is mild. However, the corrosion is very intense at high temperatures. In this case, the anodic reaction occurs on the carbon steel surface as follows:

$$Fe+4OH^- \rightarrow FeO_2^{2-}+2H_2O+2e$$

The ferrate ion (FeO_2^{2-}) formed is water soluble, hence this ion cannot form a protective passivation film. As a result, the corrosion of carbon steel is rapid.

3.1.2 Electrochemical polarization studies

The polarization of the N80 steel was performed in the 50 wt. % TKPP solution without any inhibitor at 30, 60, and 90 °C. No measurements were taken at a temperature of 120 °C due to the limitations of the device. As shown in Fig. 1, typical anodic passivation curves are observed, including active dissolution, transition, and passive regions. The corrosion potentials E_c of the N80 steel in this solution are relatively negative, approximately -940 mV at 30 °C, and E_c negatively shifts with increasing temperature. The polarization curves move into the passivation region at approximately -200, -280, and -510 mV at 30, 60, and 90 °C, respectively. Meanwhile, the anodic current decreases by a factor of 10^2 or 10^3, which indicates that the anodic reaction has slowed enough that the steel

becomes passive. For more noble potentials, the currents increase again, which can be attributed to the oxygen evolution as follows:

$$4OH^- \rightarrow O_2 + 2H_2O + 4e$$

Additionally, as shown in Fig. 1, the polarization curves shift to the right as the temperature increases, indicating that elevated temperature promotes the anodic reaction of the electrode and finally causes an increase in the corrosion rate of the steel.

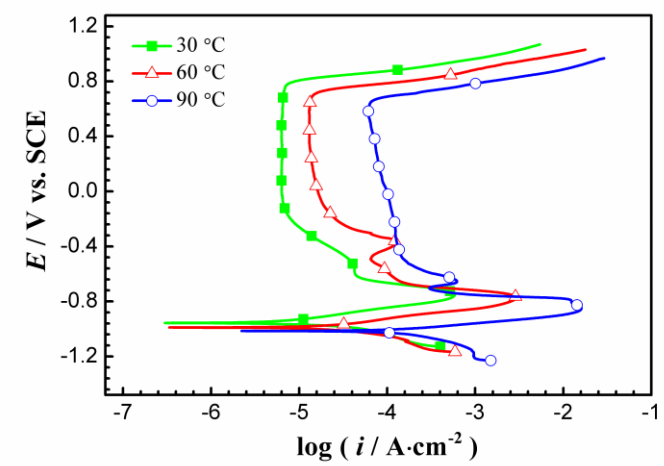

Figure 1. Polarization curves for N80 steel in 50 wt. % TKPP solution without an inhibitor at different temperatures

From the anodic polarization curves, secondary dissolution and passivation phenomena are observed, especially at 60 and 90 °C. This observation means that the chemical reaction on the surface of carbon steel may be more complex and remains to be studied further in the future.

Table 2. Electrochemical parameters of N80 steel in 50 wt. % TKPP solution without an inhibitor at different temperatures

Temperature (°C)	β_a (mV/dec)	β_c (mV/dec)	i_c (μA/cm^2)	E_c (mV vs. SCE)	Corrosion rate (mpy)
30	69.2	-95.1	4.1	-940.3	1.9
60	81.9	-95.2	11.7	-978.6	5.4
90	67.3	-172.1	184.6	-1097.2	85.3

The corrosion rates of N80 steel and other electrochemical parameters, determined by fitting the weak polarization zones of the curves using the Gauss-Newton method, are listed in Table 2, where β_a is the anodic Tafel slope, β_c is the cathodic Tafel slope, E_c is the corrosion potential, and i_c is the corrosion current density. As shown in Table 2, the corrosion rate increases as the temperature rises. The results are in good agreement with those obtained by the weight-loss method, although the absolute values of the corrosion rates are different, which is likely due to the difference in test method [10].

3.2 Evaluation of corrosion inhibitors by the weight loss method

According to the literature, some compounds such as molybdate, tungstate, dichromate, nitrite, phosphate, silicate, and acrylamide are effective corrosion inhibitors in corrosive solutions [11]. Vanadates (sodium vanadate and metavanadate), as oxidizing inhibitors, have excellent corrosion inhibition performance for steel in hot potassium carbonate solutions [12]. Therefore, their corrosion inhibition performances were evaluated using the weight loss method in the test solution at 120 °C. The results are displayed in Table 3.

Table 3. Corrosion rates of N80 steel obtained by the weight loss method in 50 wt. % TKPP solutions with various corrosion inhibitors at 120 °C

Corrosion inhibitor	Conc. of inhibitor (wt. %)	Corrosion rate (mpy)	IE (%)
blank	0	731.0	-
Na_2MoO_4	0.5	114.9	84.28
	1.0	116.8	84.02
Na_2WO_4	0.5	95.7	86.70
	1.0	101.2	86.18
$Na_6O_{18}P_6$	1.0	192.5	73.66
C_3H_5NO	0.5	105.7	85.67
	1.0	126.8	82.65
K_2CrO_4	1.0	0.4	99.73
$NaNO_2$	0.5	44.7	93.88
	1.0	42.2	94.22
Na_2SiO_3	0.5	101.5	86.04
	1.0	87.6	88.02
Na_3VO_4	1.0	1.3	99.07
$NaVO_3$	0.5	1.1	99.85

As shown in Table 3, molybdate, tungstate, phosphate, silicate and acrylamide show weak inhibition abilities in the solution at the test concentrations. Nitrite exhibits moderate inhibition efficiencies. Notably, chromate shows excellent corrosion inhibition at a concentration of 1.0 wt. %. The corrosion rate of steel decreases to 0.4 mpy, and the inhibition efficiency rises to 99.73 %. However, chromates are defined as carcinogenic substances with extremely high levels of toxicity and highly negative effects on the human body and the environment. For this reason, chromate is not further investigated in the following experiments.

Likewise, vanadates including vanadate (Na_3VO_4) and metavanadate ($NaVO_3$) exhibit excellent corrosion inhibition in the system investigated. The corrosion rate is reduced to 1.3 mpy at a concentration of 1.0 wt. % Na_3VO_4 at 120 °C.

Table 4. Corrosion rates of N80 steel obtained by the weight loss method in 50 wt. % TKPP solutions with 0.5 wt. % $NaVO_3$ at different temperatures

Temperature (°C)	Corrosion rate (mpy)	IE (%)
30	0.09	99.98
60	0.15	99.97
90	0.22	99.96

$NaVO_3$ also shows excellent corrosion inhibition at lower temperatures. As shown in Table 4, the corrosion rates are determined to be 0.09, 0.15 and 0.22 mpy at 30, 60 and 90 °C, respectively, with the addition of 0.5 wt. %.

3.3 Inhibition mechanism of $NaVO_3$

3.3.1 Polarization curves

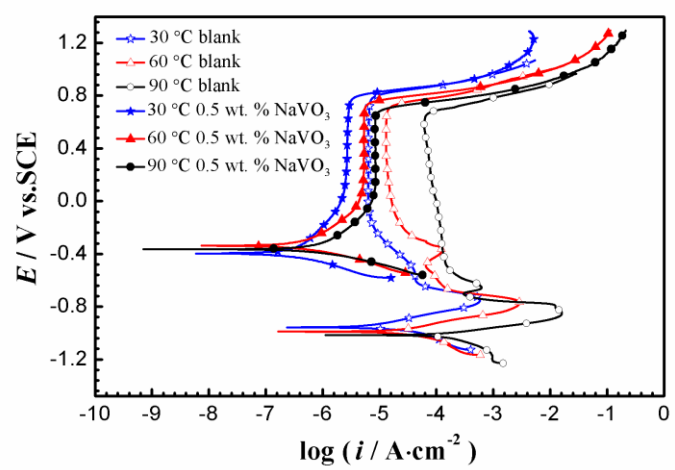

Figure 2. Polarization curves for the N80 steels in 50 wt. % TKPP solutions with and without 0.5 wt. % $NaVO_3$ at 30, 60 and 90 °C

Because it is easily available, metavanadate is chosen for study of its inhibition mechanism. The polarization curves for N80 steel in the presence of 0.5 wt % $NaVO_3$ at 30, 60 and 90 °C are shown in Fig. 2. For the convenience of comparison, the polarization curves measured in the blank solution are also shown in Fig. 2. Compared with the curves in the blank solution, the polarization curves in the presence of 0.5 wt. % $NaVO_3$ significantly shift to the left, and the corrosion potentials

and passivation potentials positively increase. Meanwhile, the active current peak in the polarization curve disappears, which means that the steel is in a passive state at the corrosion potential. The passive current density decreases by a factor of 10^1 or 10^2 in the presence of 0.5 wt. % $NaVO_3$. Therefore, these results clearly demonstrate that $NaVO_3$ could act as an anodic inhibitor and promote the passivation of steel in the solution.

The Pourbaix diagram of the Fe-H_2O system shows that carbon steel is in the corrosion region when the corrosion potential is in the range of -940 ~ -1100 mV in a solution with a pH of 14 [13]. After the addition of a corrosion inhibitor, the corrosion potential of carbon steel shifts to approximately -400 mV, which is in the passivation region, consistent with the results of this work.

Table 5. Electrochemical parameters of N80 steel in 50 wt. % TKPP solutions with 0.5 wt. % $NaVO_3$ at different temperatures

Temperature (°C)	β_a (mV/dec)	β_c (mV/dec)	i_c (μA/cm^2)	E_c (mV vs. SCE)	Passive current density (μA/cm^2)
30	101.6	-66.2	0.161	-398.0	2.77
60	117.3	-70.5	0.280	-338.1	5.24
90	143.4	-72.1	0.545	-364.4	8.20

Table 5 shows that with increasing temperature, the passive current density increases gradually, indicating that elevated temperature leads to more intense corrosion reactions.

Table 6. Electrochemical parameters obtained from polarization measurements of N80 steel in 50 wt. % TKPP solutions with various concentrations of $NaVO_3$ at 90 °C

Conc. of $NaVO_3$ (wt. %)	β_a (mV/dec)	β_c (mV/dec)	i_c (μA/cm^2)	E_c (mV vs. SCE)	Corrosion rate (mpy)
0.15	134.7	-74.6	1.26	-440	0.60
0.25	132.8	-75.1	0.77	-430	0.35
0.5	117.3	-70.5	0.28	-390	0.12
1.0	138.3	-73.5	0.82	-320	0.39

The polarization curves were also measured in solutions with different concentrations of $NaVO_3$ at 90 °C. The variation in inhibition efficiency with inhibitor concentration is shown in Fig. 3. The electrochemical parameters are given in Table 6. These results clearly indicate that the inhibition efficiency of $NaVO_3$ increases dramatically with increasing concentration in the concentration range of 0-0.5 wt. %. The inhibition efficiency tends to be diminished when the concentration increases from 0.5 to 1.0 wt. %. Hence, the optimum concentration of $NaVO_3$ is 0.5 wt. % at 90 °C.

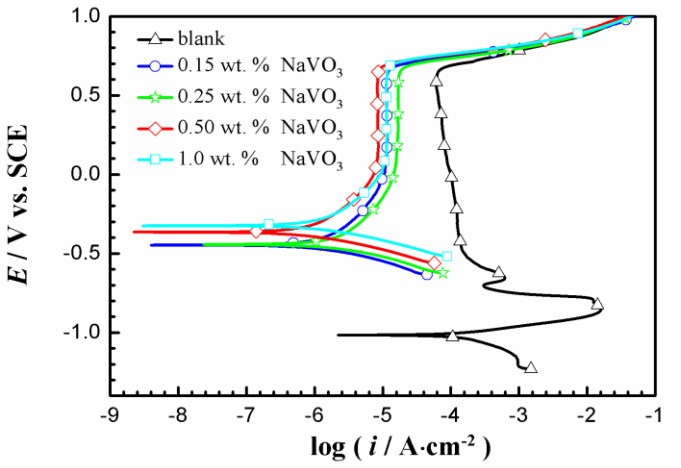

Figure 3. Polarization curves for N80 steel in 50 wt. % TKPP solutions containing various concentrations of $NaVO_3$ at 90 °C

3.3.2 EIS

EIS measurements of the N80 steel in the solutions with and without 0.5 wt. % $NaVO_3$ at 30, 60 and 90 °C were performed at different temperatures, and the resulting Nyquist plots are shown in Fig. 4(a) and (b).

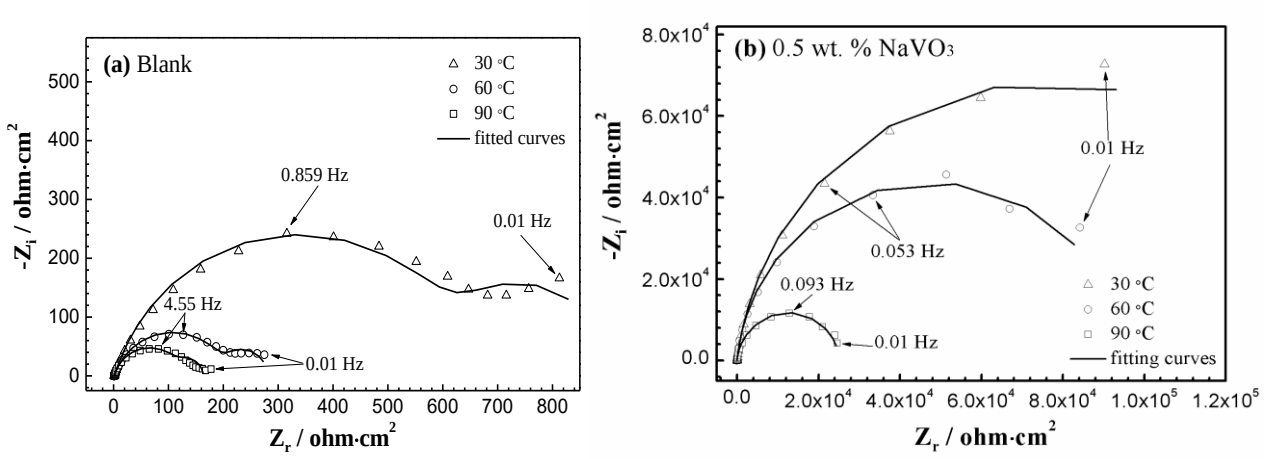

Figure 4. Nyquist plots for N80 steel in 50 wt. % TKPP solutions without (blank) and with 0.5 wt % $NaVO_3$ at 30, 60 and 90 °C

Fig. 4 shows that all the Nyquist plots have a depressed semicircle with a center under the real axis in the high frequency range, which is characteristic of solid electrodes and is attributed to the roughness and other heterogeneities of the electrode [14-15]. The diameters of the semicircle increase by approximately 2 orders of magnitude in the presence of 0.5 wt. % $NaVO_3$, indicating that $NaVO_3$ can dramatically inhibit the corrosion of N80 steel in the test solution.

Two equivalent circuits shown in Fig. 5 are proposed to fit the EIS plots with and without $NaVO_3$, where R_s is the solution resistance, R_{ct} is the charge transfer resistance, and Q_{dl} is the constant

phase element instead of a pure double-layer capacitor to give a more accurate fit [16]. R_{cp} and C_{cp} are the resistance and capacitance of the corrosion product layer, respectively.

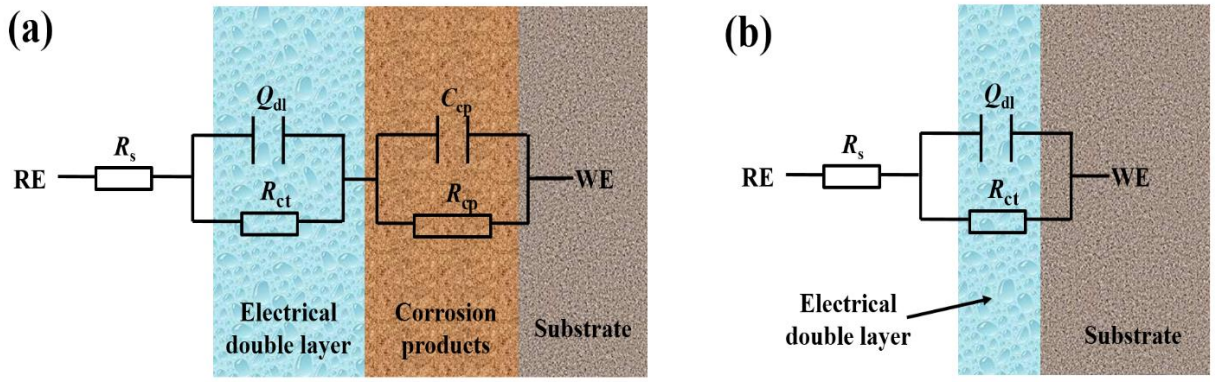

Figure 5. Equivalent circuits used to fit the Nyquist plots with and without $NaVO_3$

Table 7. Electrochemical impedance parameters and inhibition efficiencies obtained from EIS measurements for N80 steel in solution with and without 0.5 wt. % $NaVO_3$ at different temperatures

Temperature (°C)	Conc. of $NaVO_3$ (wt. %)	R_s (Ω cm^2)	R_{ct} (Ω cm^2)	Q_{dl}		C_{dl} (μF cm^{-2})	R_{cp} (Ω cm^2)	C_{cp} (μF cm^{-2})	IE (%)
				Y (μΩ^{-1}·cm^{-2}·S^n)	n				
30	0	1.616	6.49×10^2	457.5	0.7956	334.9	251	3780	-
	0.5	4.393	1.53×10^5	66.47	0.9269	79.81	-	-	99.41
60	0	1.265	2.07×10^2	727.3	0.7784	424.2	72.5	6795	-
	0.5	2.426	9.56×10^4	50.81	0.9434	55.86	-	-	99.71
90	0	1.250	1.22×10^2	651.8	0.8198	373.6	40.3	2363	-
	0.5	0.940	2.52×10^4	83.40	0.9518	86.60	-	-	99.36

The fitted results are listed in Table 7. The values of C_{dl} decrease significantly in the presence of vanadate, which is attributed to the formation of a passive film on the steel surface. R_{ct} increases by approximately 2 to 3 orders of magnitude in the presence of 0.5 wt. % $NaVO_3$, meaning that corrosion is strongly inhibited and all the IE are greater than 99 %, which further confirms that $NaVO_3$ is an excellent corrosion inhibitor.

3.3.3 SEM and XPS

After the weight loss tests at different temperatures, the N80 steel specimens were taken out of solution, slightly rinsed with distilled water, and dried with a hot air stream. Subsequently, the morphology of the corroded surfaces was observed with SEM. XPS measurements were also performed to detect the presence of vanadium at the surface and possibly its oxidation state.

Fig. 6 shows the surface morphology of the N80 steel corroded at different temperatures without and with 0.5 wt. % $NaVO_3$. As shown in Fig. 6, the corrosion is mild at 30 and 60 °C without the inhibitor but becomes severe at 90 °C. Moreover, more severe corrosion occurs at 120 °C, and the

surfaces of the specimens are covered by a large amount of muddy corrosion product. In contrast, the specimens in the solution containing 0.5 wt. % $NaVO_3$ are well protected at various temperatures.

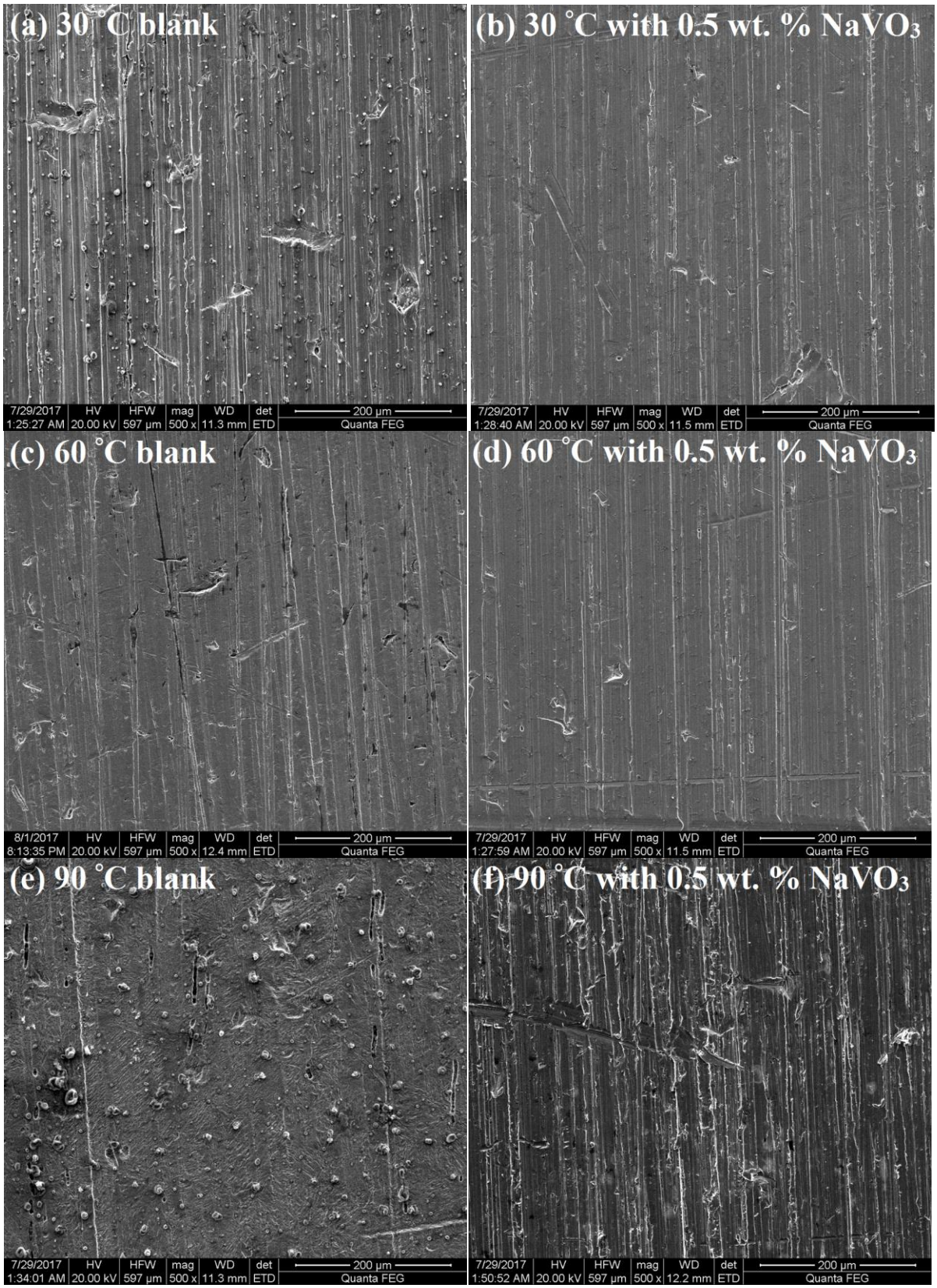

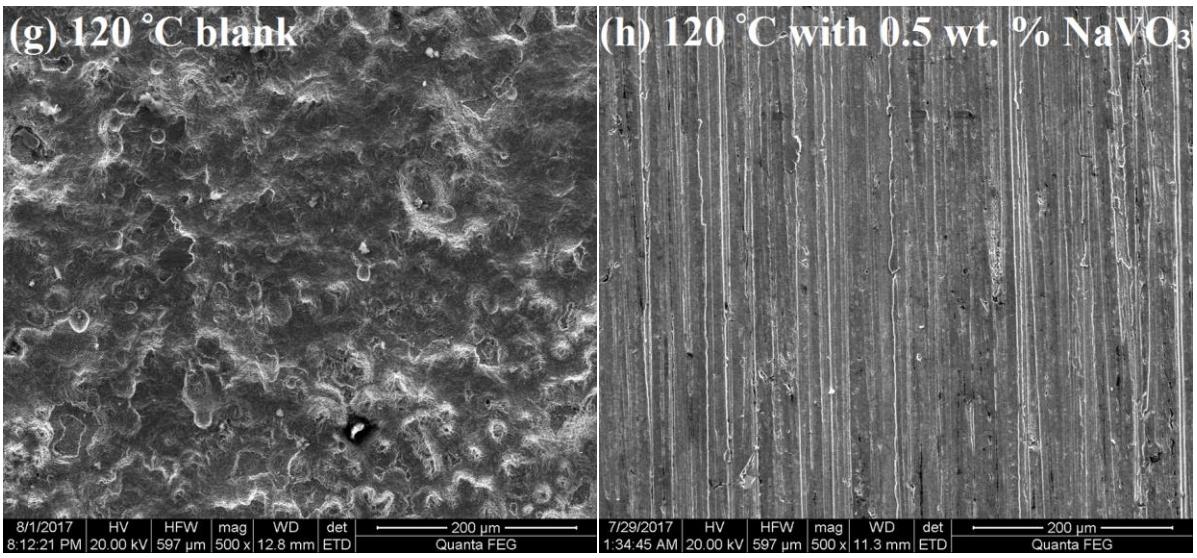

Figure 6. Surface morphologies of the N80 steel corroded at different temperatures without and with 0.5 wt. % $NaVO_3$

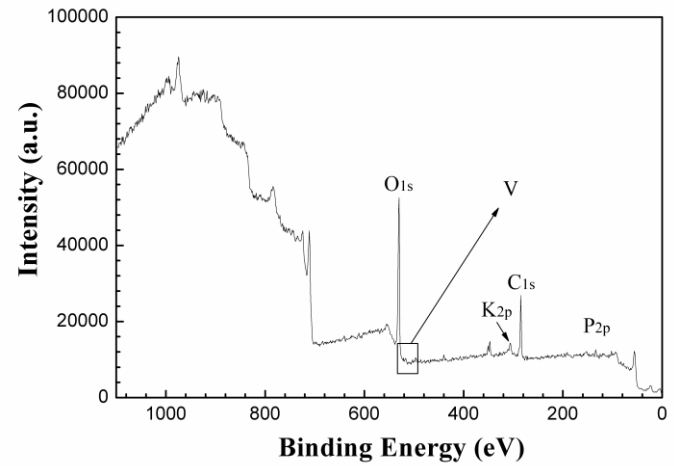

Figure 7. Wide-scan XPS spectrum of N80 steel corroded in solution with 0.5 wt. % $NaVO_3$ at 90 °C for 3 days

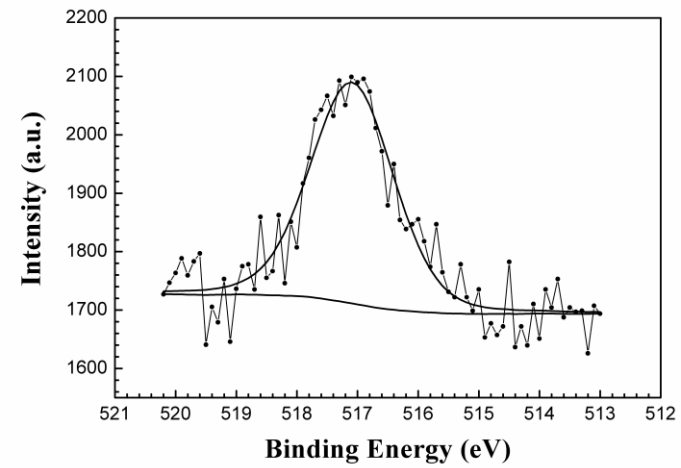

Figure 8. High-resolution XPS spectrum of V2p of N80 steel corroded in solution with 0.5 wt. % $NaVO_3$ at 90 °C for 3 days

V is not detected by the EDS performed during SEM, which is likely attributed to only trace amounts of V existing on the steel surface.

For the sake of economizing space, only the XPS results of the specimens corroded in 50 wt. % TKPP solution with 0.5 wt. % $NaVO_3$ at 90 °C are provided. Fig. 7 provides evidence for the presence of C, O, K, P and V on the steel surface. Compared with the other elements detected, the intensity of the V peak is very low. Similar results were also observed by Iannuzzi and Frankel [17]. Fig. 8 shows the high-resolution XPS spectrum of V2p. The vanadium peak is at a binding energy of 517.4 eV, which corresponds to a 5+ oxidation state [18].

4. CONCLUSIONS

(1) The corrosion rate of N80 steel increases with increasing temperature in 50 wt. % TKPP solution in the absence of an inhibitor. The corrosion rate is moderate in the low temperature range but increases dramatically when the temperature exceeds 90 °C. In particular, the corrosion rate reaches 731 mpy at 120 °C.

(2) The results from the electrochemical measurements show that elevated temperature significantly increases the corrosion rate. The anodic reaction is increased, but the cathodic reaction is influenced to a greater extent given the decrease in the open circuit potential.

(3) Among the inhibitors investigated, vanadate and dichromate exhibit significant corrosion inhibition abilities in solution. $NaVO_3$ possesses the capacity to reduce the corrosion rate to less than 3 mpy at a concentration of 0.5 wt. % at 120 °C.

(4) The studies regarding the corrosion inhibition mechanism of $NaVO_3$ demonstrate that the inhibitor acts as an anodic inhibitor through the promotion of carbon steel passivation.

ACKNOWLEDGEMENTS
The authors would like to thank the National Natural Science Foundation of China (No. 51471021) for support of this work.

References

1. U.R. Sumaila, A.M. Cisneros-Montemayor, A. Dyck, L. Huang, W. Cheung, J. Jacquet, K. Kleisner, V. Lam, A. McCrea-Strub, W. Swartz, R. Watson, D. Zeller, D. Pauly, Can. J. Fish. *Canadian Journal of Fisheries & Aquatic Sciences*, 69 (2012) 499.
2. A. Hopkins, *Safety Science*, 39 (2011) 3.
3. J. Li, B. Zhang, Y. Wang, M. Liu, *Safety Science*, 47(2009)1107.
4. T.Ariyaratna, N. Obeyesekere, and J. Wylde. (2016). 'Development of novel inhibitor chemistries to protect metal surfaces from saturated completion fluid' in CORROSION 2016, *NACE*, Vancouver, British Columbia Canada, paper no. 7802.
5. M. Ke, R.F. Stevens, and Q. Qu. (2008). 'Novel corrosion inhibitor for high density znbr2 completion brines at high temperatures' in CORROSION 2008, *NACE*, Vancouver, New Orleans, LA, paper no. 08630.

6. R.J. Spies, A.K. Himmatramka, J.R. Smith, D.C. Thomas, *Journal of Petroleum Technology*, 35 (1983) 2.
7. N.G. Smart, R.C. Bhardwaj, J.O'M. Bockris, *Corrosion -Houston Tx-*, 48 (2012) 764.
8. J.T. Patton, W.T. Corley, *ACS Symposium Series*, 396 (1989) 636.
9. J. Zhao, G. Chen, *Electrochim Acta*, 69 (2012) 247.
10. M.A. Hegazy, M. Abdallah, H. Ahmed, *Corrosion Science*, 52 (2010) 2897.
11. J. Zhao, M. Zhang, Z. Tie,*Chemical Research in Chinese Universities*, 33 (2017) 1.
12. B.S. Zhou, J.X. Yang. (1985). 'Some studies on the critical passivation concentration of oxidizing inhibitors' *Proceedings of 6th European symposium on corrosion inhibitors*, (Ann. Univ. Ferrara, N.S., V, Suppl. 1985), p. 397.
13. M. Pourbaix, *Lectures on Electrochemical Corrosion*, Plenum Press, (1973) 98.
14. K. Jüttner, *Electrochim Acta*, 35 (1990) 1501.
15. T. Paskossy, *Journal of Electroanalytical Chemistry*, 364 (1994) 111.
16. A.V. Benedetti, P.T.A. Sumodjo, K. Nobe, P.L. Cabot, W.G. Proud, *Electrochim Acta*, 40 (1995) 2657.
17. M. Iannuzzi, G.S. Frankel, *Corrosion Science*, 49(2007)2371.
18. P. Mezentzeff, Y. Lifshitz, J.W. Rabalais, *Nuclear Inst & Methods in Physics Research B*,44 (1990) 296.